Theoretical Analysis of a passive wearable spring-clutch mechanism for reducing metabolic energy cost during human walking

Roee Keren and Yizhar Or

Faculty of Mechanical Engineering, Technion - Israel Institute of Technology. Haifa 3200003, Israel.

E-mail: `izi@technion.ac.il`

Abstract. There is a growing interest in assistive wearable devices for laden walking, with applications to civil hiking or military soldiers carrying heavy loads in outdoor rough terrains. While the solution of full powered exoskeleton is known to be heavy and energy consuming, recent works presented wearable light-weight semi-passive elements based on elastic springs engaged by timed clutches. In this work, we theoretically study the dynamics of a five-link model of a human walker with point feet. We propose a novel mechanism of a spring and two triggered clutches, which enables locking the spring with stored energy while the device's length can change freely. For a given gait of joint angles trajectories, we optimize the spring parameters and clutch timing for minimizing the metabolic energy cost. We show that a cleverly designed device can, in theory, lead to a drastic reduction in metabolic energy expenditure.

1. Introduction

The use of wearable mechanical devices for assisting human walking and load carrying has become an attractive challenge of engineering research and development over the last decade [1, 2]. Powered exoskeletons have been developed, either for rehabilitation and stroke recovery [3, 4, 5], enabling upright walking of disabled persons [6, 7, 8], or for assisting legged mobility of healthy humans [9, 10]. The latter case has several potential applications for geriatric assistance [11], or for hikers, combat soldiers [12] and maintenance crew carrying heavy loads in rough outdoor terrains [13, 14, 15, 16]. Such anthropomorphic powered exoskeletons with rigid structure are known to be heavy and consume a large amount of energy, which must be supplied by carried batteries, thus limiting long-range untethered mobility in outdoor terrains [17]. On the other hand, recent works in biomechanics and bio-robotics research communities have presented several light-weight wearable assistive devices which operate passively, or require only low-power triggering activation [18, 19, 20]. Most of these wearable devices rely heavily on elastic springs which are used in order to store and release energy, borrowing inspiration from the role of elasticity in biological legged locomotion [21]. In particular,

the recent work [22] has demonstrated a remarkable reduction of the metabolic energy expenditure during walking by using an extension spring for assisting the ankle joint at foot push-off. Another related implementation is the use of elastic suspension for load carrying [23], with various applications such as handle mechanisms [24, 25] or legged robots [26]. Backpack suspension systems have been studied experimentally in [27, 28] and analyzed theoretically in [29, 30], proving possible reduction in energy expenditure, both theoretically and experimentally.

Many of the wearable assistive devices mentioned above include triggering elements such as clutch, brake, or ratchet-pawl mechanism [31, 32, 33]. Such elements are commonly used for engagement and disengagement of the spring [22, 34], while other devices use triggering for changing the stiffness of elastic joints or at foot contact [35, 36, 37]. The fully-passive exoskeleton in [38] uses clutch-brake elements for locking the knee joint during single-support ballistic motion. While the concept of clutch-triggered elastic devices has been proven to improve energy efficiency in [22], no systematic analysis of the influence of timing the clutch triggering on the motion dynamics and energetics have been conducted. Moreover, the existing spring-clutch mechanism in [22] only enables engagement or disengagement of the spring, and does not involve a locked state of the spring with stored potential energy.

The goal of this work is to conduct optimization of such a wearable device by using a simple theoretical model. We propose a novel concept of a spring-clutches mechanism which enables locking the spring with stored energy while the device's length can change freely, and then releasing the stored elastic energy at a desired stage of the motion by re-engaging the spring. We use a simple five-link model of human bipedal walking is sagittal plane. Trajectories of gait kinematics obtained in [39] are used for theoretically analyzing the effect of the spring-clutches mechanism on metabolic energy expenditure, as defined in the formula of Margaria [40, 41]. We use distance and energy plots for guiding the selection of clutch triggering times between different states of the spring, and conduct numerical optimization of the spring's properties, triggering times, and geometric structure of the device, for minimizing the metabolic energy cost. Our theoretical analysis indicates that clever design of the device and tuning its timing can result in substantial energy saving. This work is motivated by our recent theoretical results in [42], where we incorporated a timed clutch into the two-mass theoretical model of [29] for a backpack suspension system.

2. Problem statement

We now introduce the five-link planar model, formulate the metabolic energy cost, and present our proposed spring-clutches mechanism. The five-link planar model is shown in Figure 1(a). It consists of two legs with point feet, knee and hip joints, and an upper link that represents the human's torso. The lengths l_i and masses m_i of each link are listed in Table 1 The values are adapted from the model in [39] (up to a scaling factor). The links are assumed to be thin rods with uniform mass distribution, so that the center
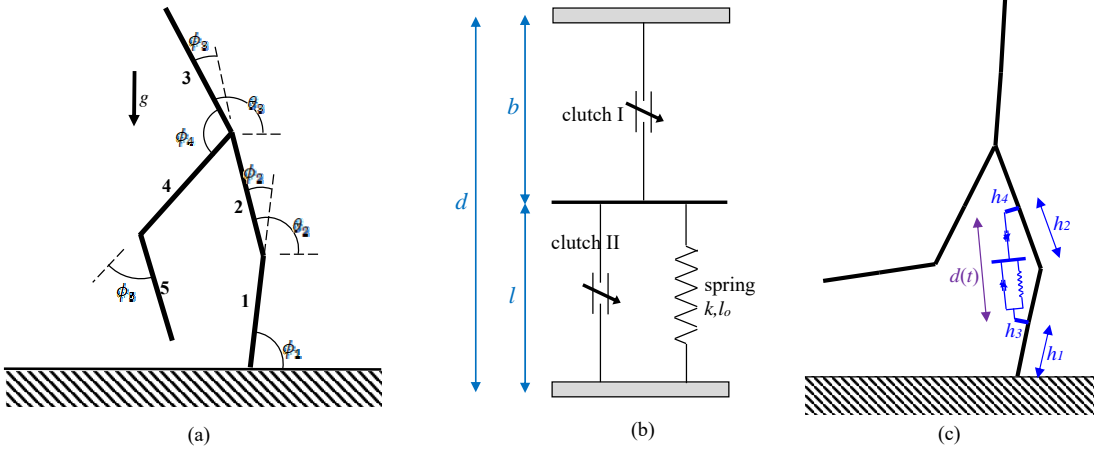
Figure 1. (a) The five-link model with notation. (b) Schematics of the proposed spring-clutches mechanism. (c) The five-link model with the spring-clutches mechanism on the stance leg.

Table 1. Physical parameters of the five-link models

Number i	Name	Mass m_i [Kg]	Length l_i [m]
1,5	shin	4.88	0.38
2,4	thigh	7.90	0.452
3	torso	54.44	0.968
	whole body	80	1.80 (upright)

of mass of each link is located at its midpoint while the moment of inertia is given by $I_i = \frac{1}{12} m_i l_i^2$. The relative angles at the joints are ϕ_i, as denoted in Figure 1(a).

The five-link model moves and makes a step where one foot touches the ground (stance foot) while the other foot swings forward. While the joint angles change over time as $\phi_i(t)$, the mechanical torque acting at each joint is $\tau_i(t)$. The mechanical power expenditure at each joint is given by

$$P_i(t) = \tau_i(t)\dot{\phi}_i(t). \tag{1}$$

The total mechanical work (energy) along a step is obtained as

$$W_{mech} = \sum_{i=1}^{5} \int_0^T P_i(t)dt. \tag{2}$$

Note that mechanical power $P_i(t)$ can be negative at some parts of the motion, leading to reduction in total energy. While this is feasible for motorized joints with energy regeneration capabilities, it is not practical for muscle activity where one has to consider *metabolic work* instead of mechanical work. This is done by considering Margaria's formula [40] which assumes different mechanical efficiencies for positive and negative work:

$$W_{met} = \sum_{i=1}^{5} \int_0^T \frac{P_i(t)}{\eta_i(t)}dt, \text{ where } \eta_i(t) = \begin{cases} 0.25 & P_i(t) \geq 0 \\ -1.2 & P_i(t) < 0 \end{cases}. \tag{3}$$

Table 2. States of the two-clutch mechanism

Clutches states	I - free	I - engaged
II - free	A. free	B. active spring
II - engaged	C. spring locked free motion	D. rigid connection

That is, positive mechanical work involves muscular energy efficiency of 25%, while absorption of negative work requires positive muscular work with "efficiency" of 120%. Therefore, the desired action of a passive wearable spring-based device is to store energy during phases of negative power and release it during phases of positive power, in order to reduce the metabolic energy expenditure of muscles. With this aim in mind, we propose the spring-clutches mechanism detailed below.

The proposed mechanism is shown in Figure 1(b). It contains an arrangement of a linear spring with stiffness k and free length l_o and two clutches (I and II) that can trigger between engaged and free states. Clutch I is connected in series to the spring, while clutch II is connected in parallel to it. The device thus has four different states (A,B,C,D), which are summarized in Table 2. State C of clutch I free and clutch II engaged is of crucial importance, since it means that the spring is locked and stores potential energy, while the endpoints of the device can move freely. This enables separation between phases of energy storage and release, which is a main difference from previous works such as [22] where stored energy had to be released immediately. This device can be connected to the biped model as shown in Figure 1(c). The main objective of this work is to find the parameters of the device's geometry, spring properties, and clutch timing in order to minimize the metabolic energy expenditure along a step, as analyzed in the next section.

3. Analysis

We now analyze the motion of the five-link model. We first introduce our reference trajectory of joint angles. Then we formulate the dynamic equations of motion and compute the mechanical and metabolic energy expenditure. Finally, we explain the operation principle of our proposed spring-clutches mechanism.

3.1. Gait kinematics

The kinematics of the walking gait is adapted from the work of Ames *et al* in [39]. They have experimentally obtained motion measurements of several human subjects during steady-state periodic walking on a treadmill. Then the data has been projected onto the five-dimensional joint space of the model shown in Figure 1(a). Since the data analysis in [39] involved averaging across several subjects, the trajectories contained some small non-uniformities such as penetration into the ground, and asymmetries between consecutive poses of double-stance contact. In order to correct these deviations,
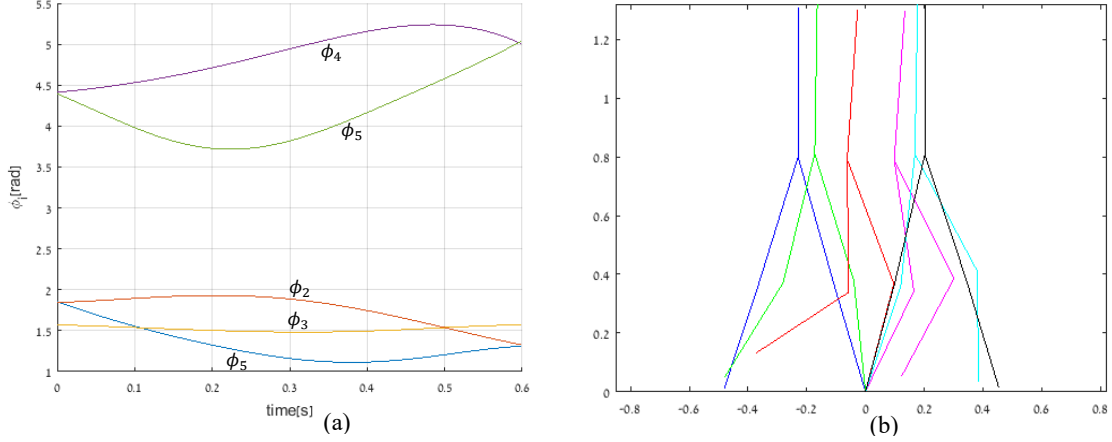
Figure 2. The chosen gait from [39] for the five-link model: (a) Joint angle trajectories. (b) Motion snapshots.

we have made slight modifications to the trajectories and then smoothened them by cubic spline interpolation. The resulting reference trajectories of the five joint angles are shown in Figure 2(a), while motion snapshots of the model along a single step are shown in Figure 2(b).

3.2. Formulation of the dynamic equations

We now present formulation of the dynamics of the five-link biped model. For convenience, we choose the generalized coordinates $\mathbf{q} = (\theta_1, \ldots \theta_5)^T$, where θ_i is the absolute orientation angle of the ith link. These angles are related to vector of relative angles at the joints $\boldsymbol{\Phi} = (\phi_1, \ldots \phi_5)^T$ through the linear transformation:

$$\mathbf{q} = \mathbf{W}\boldsymbol{\Phi}, \text{ where } \mathbf{W} = \begin{pmatrix} 1 & 0 & 0 & 0 & 0 \\ 1 & 1 & 0 & 0 & 0 \\ 1 & 1 & 1 & 0 & 0 \\ 1 & 1 & 1 & 1 & 0 \\ 1 & 1 & 1 & 1 & 1 \end{pmatrix}. \tag{4}$$

Using Lagrange's formulation of kinetic and potential energy (cf. [43]), the dynamic equations of motion for this five-link model are:

$$\frac{d}{dt}\left(\frac{\partial T}{\partial \dot{\mathbf{q}}}\right) - \frac{\partial T}{\partial \mathbf{q}} + \frac{dU}{d\mathbf{q}} = \mathbf{F}_q \tag{5}$$

The total kinetic energy T of all links is given by

$$T = \sum_{i=1}^{5} \frac{1}{2} m_i (\dot{\mathbf{r}}_i \cdot \dot{\mathbf{r}}_i) + \frac{1}{2} I_i \dot{\theta}_i^2$$

where $\mathbf{r}_i$ is the position vector of the ith link's center of mass. The potential energy of gravity and elasticity (if the spring is active) is given by

$$U = U_g + U_k = \sum_{i=1}^{5} m_i g \mathbf{r}_i \cdot \hat{\mathbf{y}} + \frac{1}{2} k \left(l(\mathbf{q}) - l_0 \right)^2$$
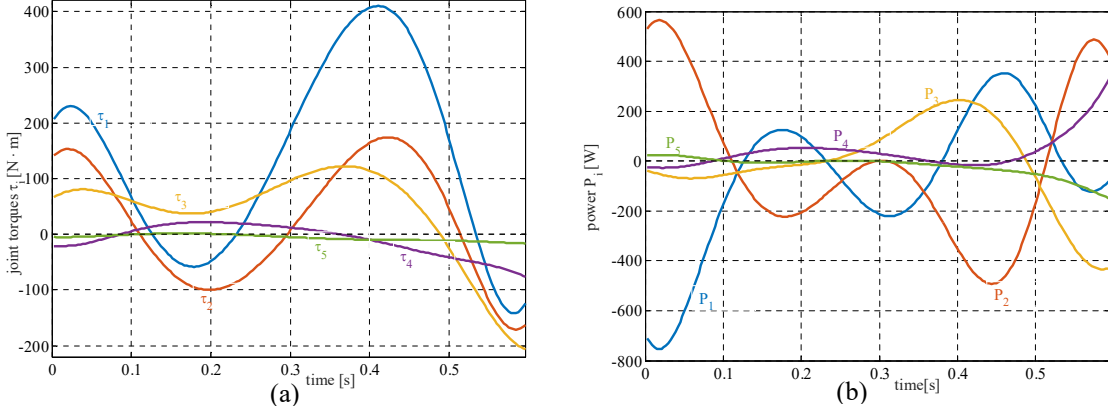
Figure 3. (a) Torques at the joints during motion $\tau_i(t)$. (b) Mechanical power at the joints during motion $P_i(t)$.

where g is the gravitational acceleration, $\hat{\mathbf{y}}$ is the upward unit vector (opposing gravity), and $l(\mathbf{q})$ is the spring's length. The term $\mathbf{F}_q$ in (5) is the vector of generalized forces generated by the joint torques. Using kinematic relations for computing the kinetic and potential energies and substituting into (5), the equation of motion can be arranged in matrix form as:

$$\mathbf{M}(\mathbf{q})\ddot{\mathbf{q}} + \mathbf{h}(\mathbf{q}, \dot{\mathbf{q}}) + \mathbf{g}(\mathbf{q}) + \mathbf{k}(\mathbf{q}) = \mathbf{W}^{-T}\boldsymbol{\tau}, \tag{6}$$

where $\mathbf{M}(\mathbf{q})$ is the system's matrix of inertia, $\mathbf{h}(\mathbf{q}, \dot{\mathbf{q}})$ is a vector of velocity-dependent inertial terms, $\mathbf{g}(\mathbf{q})$ is the vector of gravitational terms, and $\mathbf{k}(\mathbf{q})$ are elastic forces due to action of the spring, when it is active. Explicit expression for all elements of these terms are given in Table 3. On the right hand side of (6), $\boldsymbol{\tau} = (\tau_1 \ldots \tau_5)^T$ is the vector of mechanical torques at the joints. For the chosen gait $\mathbf{q}(t)$ in Figure 2, one can apply numerical differentiation in order to obtain velocities $\dot{\mathbf{q}}$ and accelerations $\ddot{\mathbf{q}}$, and then substitute into the equation of motion (6) in order to obtain the mechanical torques at the joints $\tau_i(t)$. For the nominal case without a spring, these torques are shown in Figure 3(a). Using eq. (1), the mechanical power expenditure at each joint $P_i(t)$ is then computed, as shown in Figure 3(b). The total mechanical work as defined in (2) during a step is obtained as $W_{mech} = 45.5J$. Note that the expression in (2) also accounts for negative work, and the initial and final configuration are identical up to interchanging between legs, and thus have equal potential energy. Therefore, this mechanical work only reflects the energy losses due to foot impact. On the other hand, the total metabolic energy expenditure defined in (3), which penalizes negative work, is obtained as $W_{met} = 879.7J$, which better reflects the realistic value of muscular work during a step [40].

3.3. Action of the spring-clutches mechanism

We now explain the periodic action of the spring-clutches mechanism during a step. The length of the device $d(t)$ changes during motion, see Figure 1(c). We consider two stages where the spring is active during a step, one for energy storage and one for energy release. Initially, the device is assumed to be in state C (see Table 2) where the spring is locked with initial preloading of length Δ (either positive for extended spring, or negative for compression), so that the spring's length is $l = l_o + \Delta$, and the gap $b(t)$ varies freely, see Figure 1(b). At time $t = t_1$, the device switches to state B and the spring becomes active. At this time, clutch I locks the gap length at $b = d(t_1) - (l_o + \Delta)$. The spring stores energy (in extension or compression) by changing $l(t)$, until time $t = t_2$, where the device switches back to state C. The spring's length is locked at $l' = d(t_2) - b = d(t_2) - d(t_1) + l_o + \Delta$ while the gap length $b(t)$ can now vary freely. Next, at time $t = t_3$ the device again switches to state B. The spring is activated at length l' and the gap length is locked at $b = d(t_3) - l'$. This stage of energy release is ended at time $t = t_4$, where the device switches back to state C. At this time, the spring should be locked exactly upon reaching its initial length, for periodicity. This imposes a constraint on the final time and length:

$$l(t_4) = l_o + \Delta \Rightarrow d(t_4) - d(t_3) = d(t_1) - d(t_2). \tag{7}$$

Optimization of clutch timing and spring's parameters for minimzing metabolic energy expenditure is conducted next.

Table 3. Explicit expressions from the dynamic equations (6)

$M_{11} = I_1 + I_2 + I_3 + I_4 + I_5 + l_1{}^2 \left(\frac{1}{4} m_1 + m_2 + m_3 + m_4 + m_5\right)$

$M_{12} = M_{21} = I_2 + I_3 + I_4 + I_5 + l_1 l_2 \cos(\theta_1 - \theta_2) \left(\frac{1}{2} m_2 + m_3 + m_4 + m_5\right)$

$M_{13} = M_{31} = I_3 + I_4 + I_5 + \frac{1}{2} m_3 l_1 l_3 \cos(\theta_1 - \theta_3), \quad M_{14} = M_{41} = I_4 + I_5 + l_1 l_4 \cos(\theta_1 - \theta_4) \left(\frac{1}{2} m_4 + m_5\right)$

$M_{15} = M_{51} = I_5 + \frac{1}{2} m_5 l_1 l_5 \cos(\theta_1 - \theta_5), \quad M_{22} = I_2 + I_3 + I_4 + I_5 + l_2{}^2 \left(\frac{1}{4} m_2 + m_3 + m_4 + m_5\right)$

$M_{23} = M_{32} = I_3 + I_4 + I_5 + \frac{1}{2} m_3 l_2 l_3 \cos(\theta_2 - \theta_3), \quad M_{24} = M_{42} = I_4 + I_5 + l_2 l_4 \cos(\theta_2 - \theta_4) \left(\frac{1}{2} m_4 + m_5\right)$

$M_{25} = M_{52} = I_5 + \frac{1}{2} m_5 l_2 l_5 \cos(\theta_2 - \theta_5), \quad M_{33} = I_3 + I_4 + I_5 + \frac{1}{4} m_3 l_3{}^2, \quad M_{34} = M43 = I_4 + I_5$

$M_{44} = I_4 + I_5 + l_4{}^2 \left(\frac{1}{4} m_4 + m_5\right), \quad M_{45} = I_5 + \frac{1}{2} m_5 l_4 l_5 \cos(\theta_4 - \theta_5), \quad M_{55} = I_5 + \frac{1}{4} m_5 l_5{}^2$

$\mathbf{h}(\mathbf{q}, \dot{\mathbf{q}}) =$

$$\begin{pmatrix} \frac{l_1}{2}\left((m_2+2m_3+2m_4+2m_5) l_2 \sin(\theta_1-\theta_2) \dot{\theta}_2^2 + m_3 l_3 \sin(\theta_1-\theta_3) \dot{\theta}_3^2 + (m_4+2m_5) l_4 \sin(\theta_1-\theta_4) \dot{\theta}_4^2 + m_5 l_5 \sin(\theta_1-\theta_5) \dot{\theta}_5^2\right) \\ \frac{-l_2}{2}\left((m_2+2m_3+2m_4+2m_5) l_1 \sin(\theta_1-\theta_2) \dot{\theta}_1^2 - m_3 l_3 \sin(\theta_2-\theta_3) \dot{\theta}_3^2 - (m_4+2m_5) l_4 \sin(\theta_2-\theta_4) \dot{\theta}_4^2 - m_5 l_5 \sin(\theta_2-\theta_5) \dot{\theta}_5^2\right) \\ -\frac{l_3 m_3}{2}\left(l_1 \sin(\theta_1-\theta_3) \dot{\theta}_1^2 + l_2 \sin(\theta_2-\theta_3) \dot{\theta}_2^2\right) \\ -\frac{l_4}{2}\left((m_4+2m_5) \sin(\theta_1-\theta_4) l_1 \dot{\theta}_1^2 + (m_4+2m_5) l_2 \sin(\theta_2-\theta_4) \dot{\theta}_2^2 - m_5 l_5 \sin(\theta_4-\theta_5) \dot{\theta}_5^2\right) \\ -\frac{l_5 m_5}{2}\left(l_1 \sin(\theta_1-\theta_5) \dot{\theta}_1^2 + l_2 \sin(\theta_2-\theta_5) \dot{\theta}_2^2 + l_4 \sin(\theta_4-\theta_5) \dot{\theta}_4^2\right) \end{pmatrix}$$

$$\mathbf{g}(\mathbf{q}) = \begin{pmatrix} g l_1 \cos(\theta_1)(0.5 m_1 + m_2 + m_3 + m_4 + m_5) \\ g l_2 \cos(\theta_2)(0.5 m_2 + m_3 + m_4 + m_5) \\ g l_3 \cos(\theta_3) 0.5 m_3 \\ g l_4 \cos(\theta_4)(0.5 m_4 + m_5) \\ g l_5 \cos(\theta_5) 0.5 m_5 \end{pmatrix}, \quad \mathbf{k}(\mathbf{q}) = \begin{pmatrix} -k\left(l_0 + b - \frac{1}{2} u_1\right) \frac{u_2}{u_1} \\ k\left(l_0 + b - \frac{1}{2} u_1\right) \frac{u_2}{u_1} \\ 0 \\ 0 \\ 0 \end{pmatrix}$$

$u_1 = \sqrt{(l_1 \cos\theta_1 + l_2 \cos\theta_2 + 2h_3 \sin\theta_1 - 2h_4 \sin\theta_2)^2 + (l_1 \sin\theta_1 + l_2 \sin\theta_2 - 2h_3 \cos\theta_1 + 2h_4 \cos\theta_2)^2}$

$u_2 = 2h_3 h_4 \sin(\theta_1 - \theta_2) - 0.5 l_1 l_2 \sin(\theta_1 - \theta_2) + h_3 l_2 \cos(\theta_1 - \theta_2) + h_4 l_1 \cos(\theta_1 - \theta_2)$
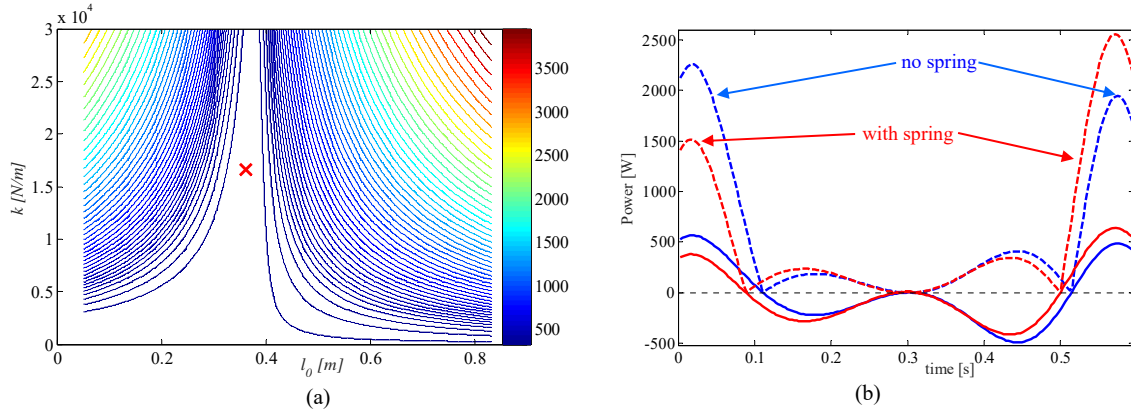
Figure 4. (a) Contour plot of metabolic energy expenditure as a function of spring parameters k, l_o. (b) Comparison of mechanical (solid curves) and metabolic (dashed) power at the knee joint for the five-link model, with and without spring.

4. Optimization of spring-clutch mechanism

We now show a series of stages for optimizing the parameter values of the spring-clutches device in order to minimize the metabolic energy expenditure. While the optimal choices are obtained numerically, the process is guided by physical intuition, as explained next.

4.1. Optimal spring without clutch triggering

The first step is adding a fully active spring without clutch triggering. We seek for the optimal combination of spring stiffness k and free length l_o that result in minimal metabolic energy over the given gait. This is done numerically by discretizing the two parameters over a 50×50 grid, within the ranges $k \in (0, 30000)N/m$ and $l_o \in (0.05, 0.83)m$, substituting the gait $\mathbf{q}(t)$ into the dynamic equation (6), and computing the metabolic cost according to (3) via quadrature integration. The results are then interpolated using cubic spline for refinement of the grid resolution to 200×200. Nominal values for the device's position are chosen as $h_1 = 0.5l_1$, $h_2 = 0.5l_2$ and $h_3 = h_4 = 0.05m$, see Figure 1(c). The results are shown in Figure 4(a) as a contour plot of the metabolic energy as a function of k and l_o. The optimal choice, marked in '×', is obtained as $k = 17,000N/m$, $l_o = 0.36m$. Figure 4(b) plots the mechanical (solid curves) and metabolic (dashed curves) power expenditure at the knee joint, with and without the spring. Note that the power expenditure with spring is lower than the power without spring at some parts of the motion, and higher at other parts. The total metabolic energy at the knee joint with the spring is $330.9J$. This amounts to 3.75% saving of the knee joint's metabolic work, and only 1.47% saving out of the total metabolic energy expenditure of the entire biped model during a step. The main reason for the poor energy saving is the fact that the time profile of the spring's energy storage and release is not synchronized with that of the joint's mechanical power. This can be significantly improved by using clutch triggering, as explained next.
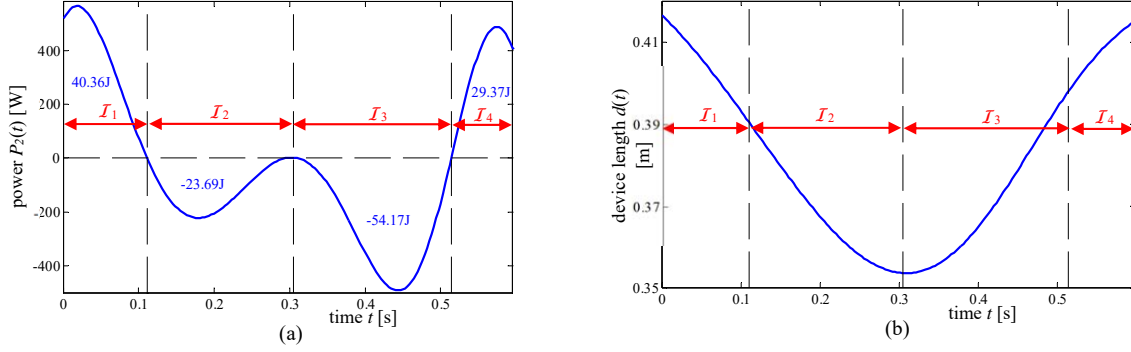
Figure 5. (a) Mechanical power at the knee joint $P_2(t)$ as a function of time. (b) Device length $d(t)$ as a function of time. Decomposition into four time intervals $\mathcal{I}_1 \ldots \mathcal{I}_4$ according to signs of $P_2(t)$ and $\dot{d}(t)$.

4.2. Using energy-distance graphs

In order to examine the best way to trigger the spring's clutches, one has to study the time profiles of the knee joint's mechanical power $P_2(t)$, combined with the device length $d(t)$ during the step, which are given in Figure 5(a) and 5(b), respectively. The time duration of the step is divided into four consecutive time intervals $\mathcal{I}_1 ... \mathcal{I}_4$, according to the sign of the mechanical power and the sign of the time rate $\dot{d}(t)$, i.e. extension or compression of the spring. Values of the positive and negative energy areas are given in 5(a). From the metabolic efficiencies in (3), it is concluded that the desired behavior of the spring is storing energy at times of negative work (time intervals $\mathcal{I}_2$ or $\mathcal{I}_3$) and releasing energy at times of positive work (intervals $\mathcal{I}_1$ or $\mathcal{I}_4$). However, the conditions for energy storage or release also depend on the behavior of $d(t)$, or more specifically on time derivative of the potential elastic energy $\dot{U}_k(t)$. Energy storage (release) is possible only if $(l(t) - l_o)\dot{l}(t)$ is negative (positive). From combining the information of Figures 5(a)-(b), one concludes that when the spring is in compression, $l < l_o$, it is possible to store energy during interval $\mathcal{I}_2$, lock the spring, and then release energy during interval $\mathcal{I}_4$. On the other hand, if the spring is in extension, $l > l_o$, it is possible to store energy during interval $\mathcal{I}_3$, lock the spring for the entire phase of foot swing, and then release energy during interval $\mathcal{I}_1$ of the next step. This observation enables obtaining an ultimate upper bound on possible energy saving, by subtracting the corresponding areas of negative mechanical work from those of positive work, and then dividing by the efficiency η which depends on the sign of the total work according to (3). It is found that the ultimate bound on energy saving for a spring in compression (area of $\mathcal{I}_4$ minus area of $\mathcal{I}_2$) is 33.3% of the metabolic work in the knee joint, whereas a spring in extension can save up to 56.7% (area of $\mathcal{I}_1$ minus area of $\mathcal{I}_3$). Thus, we conclude that the latter option of spring in extension is superior for the given gait.
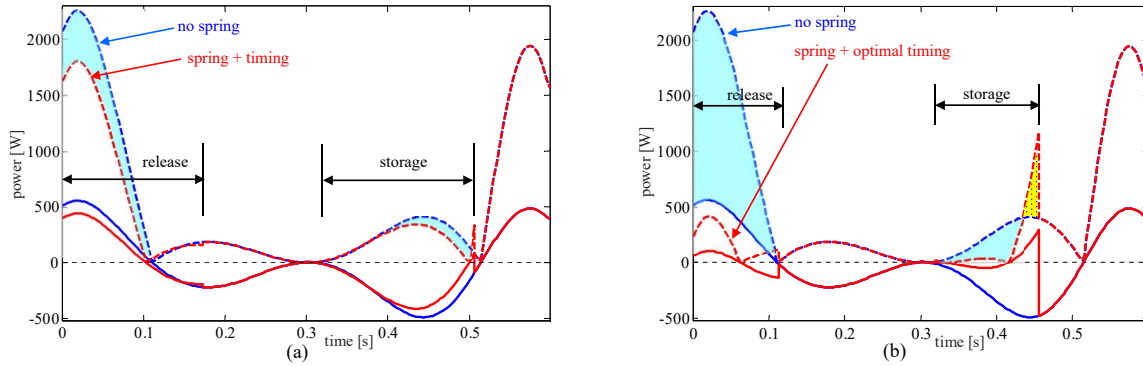
Figure 6. Mechanical (solid) and metabolic (dashed) power at the knee joint $P_2(t)$ as a function of time for: (a) naive selection of clutch timing, and (b) optimized spring and timing parameters, both compared with the nominal case without spring. Shaded regions correspond to energy saving. Small dotted region denotes excessive expended energy.

4.3. Naive selection of clutch triggering times

We now demonstrate a "naive" selection of the clutch triggering times based on the time plots of $P_2(t)$ and $d(t)$. We use the same spring parameters that have been chosen in the previous stage, whose values are $k = 17,000 N/m$ and $l_o = 0.36m$. Based on the observations above, we adopt the option of "spring in extension", hence we choose to use the time interval $\mathcal{I}_3$ for energy storage and the time interval $\mathcal{I}_1$ of the next step for energy release. Therefore, triggering times for the energy storage phase are chosen as $t_1 = 0.305s$ and $t_2 = 0.514s$, which are the endpoints of $\mathcal{I}_3$. Since $l_o > d(t_1)$, we are forced to choose $b(t_1) = 0$, hence the spring is initially in *compression* for a short time, rather than extension. Energy release is done at interval $\mathcal{I}_1$ of the next step, hence we choose $t_3 = 0$. The end of this stage is then determined according to the constraint (7) as $t_4 = 0.176$, which exceeds into the beginning of interval $\mathcal{I}_2$. Figure 6(a) plots the mechanical and metabolic power at the knee joint with and without the spring. The shaded areas in the plot denote the energy saving relative to the nominal case without a spring. With these timing parameters, the metabolic energy expenditure at the knee joint is reduced to $297.4J$, which gives saving of 13.5% relative to nominal case without a spring. The figure clearly indicates that the energy performance of the device can be further improved if the spring and timing parameters are more carefully chosen. In particular, the spring's stiffness k should be increased and the free length l_o should be decreased in order to increase the amount of energy storage and release.

4.4. Optimization of spring and timing parameters

We now conduct a simple numerical optimization of the device's parameters: spring stiffness k, initial preload Δ, and switching times of the energy storage stage t_1, t_2. For simplicity, the beginning of release stage is kept at $t_3 = 0$, and its end time t_4 is dictated according to the constraint (7). The optimization is conducted numerically by

discretizing the parameters $\{k, \Delta, t_1, t_2\}$ within a grid of size $40 \times 9 \times 9 \times 9$. For each parameter combination, we obtain the mechanical torques from (6) and intergate the metabolic power using (3), where the spring activation is determined by its triggering times and the initial preload Δ. The optimal parameter values are obtained as $k = 76000 N/m$, $\Delta = 0.00625 m$, $t_1 = 0.319 s$ and $t_2 = 0.459$. The resulting minimal metabolic energy expenditure at the knee joint is $196.6 J$, which gives 42.7% saving compared to the nominal case without spring. Figure 6(b) plots the mechanical and metabolic power at the knee joint with and without the device. The shaded regions in the plot correspond to energy saving relative to the nominal case without the spring, while the small dotted region corresponds to excessive expended energy. One can clearly see a drastic improvement compared to the "naive" selection of triggering times shown in Figure 6(a). Nevertheless, further improvement can be achieved if one uses a more refined variation of the parameters while also accounting for the geometry of the device, as studied next.

4.5. Optimized device geometry

Finally, we examine the influence of adding moderate changes in the geometry parameters of the device $h_1 \ldots h_4$, which determine the attachment points of the device relative to the thigh and shin links, see Figure 1(c). We conduct a combined optimization of all parameters using MATLAB's function **fmincon** for constrained mutli-variable minimization. The parameters, their chosen upper and lower bounds, nominal initial guess, and the resulting optimal values are all given in Table 4. Figure 7(a) plots the mechanical and metabolic power at the knee joint with optimized device, compared to the nominal case without the spring. The shaded regions in the plot correspond to energy saving relative to the nominal case without the spring, while the small dotted region corresponds to excessive expended energy. The resulting metabolic energy expenditure at the knee joint is $181.4 J$, which gives 47% saving compared to the nominal case without spring. This gives a significant improvement of 7% in energy saving due to allowing bounded changes in the locations $h_1 \ldots h_4$ from their nominally chosen values. A sketch of the five-link model with the energy-optimal geometry is shown in Figure 7(b). Note that the optimal values of $h_1 \ldots h_4$ shown in Table 4 were found to be at their upper or lower bounds. The values of these bounds were chosen arbitrarily in some moderate range, so that the device's dimensions do not exceed too much beyond the body in a way that may cause discomfort. This suggests that the energy performance could be improved further if one imposes precise practical considerations on the mechanical and ergonomic design of the device's geometry, which are beyond the scope of this work. Finally, we note that the numerical optimization algorithm has been observed to be somewhat sensitive with respect initial guesses, and converged to slightly different values with small differences in the energy cost. The chosen solution given above reflects the best result out of several initial guesses, but should be regarded as a local optimum only. A systematic search for a provably global optimum, which might be a complicated

Table 4. Numerical optimization of device parameters - summary

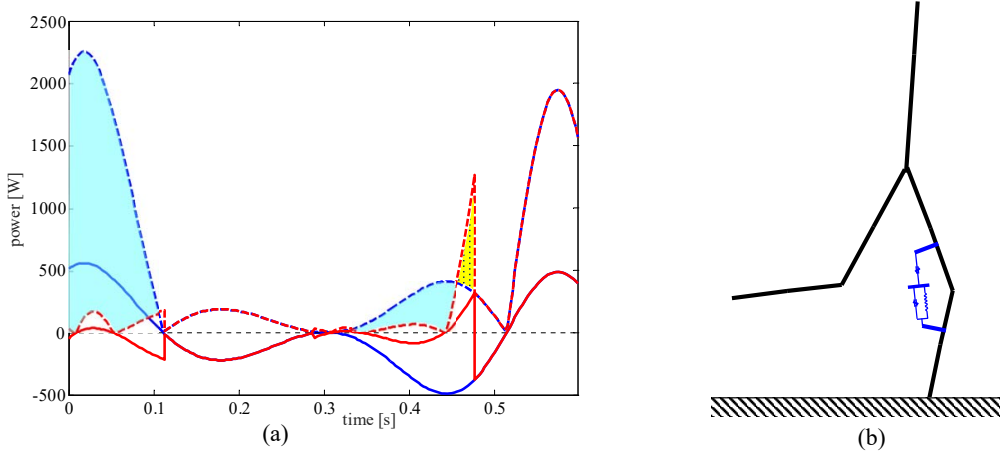| parameter	$k\ [N/m]$	$\Delta\ [m]$	$t_1\ [s]$	$t_2\ [s]$	h_1	h_2	$h_3\ [m]$	$h_4[m]$
lower bound	1000	-0.01	0.289	0.438	$0.35l_1$	$0.35l_2$	0.02	0.02
upper bound	120,000	0.05	0.375	0.524	$0.65l_1$	$0.65l_2$	0.08	0.08
initial guess	110,000	0.006	0.31	0.48	$0.5l_1$	$0.5l_2$	0.05	0.05
optimum	35,300	0.018	0.289	0.479	$0.649l_1$	$0.35l_2$	0.08	0.08

Figure 7. (a) Mechanical (solid) and metabolic (dashed) power at the knee joint $P_2(t)$ as a function of time, under optimized geometry, spring and timing parameters, compared with the nominal case without spring. Shaded regions correspond to energy saving. Small dotted region denotes excessive expended energy. (b) Sketch of the five-link model with the energy-optimal device geometry

task with extensive run-time requirements, is also beyond the scope of the current work.

4.6. Discussion

We have conducted a series of optimization stages of spring properties, clutch timing, and geometric locations. Energy saving performance in each optimization stage are summarized in Table 5. It can be seen that the concept of adding the spring and clutch triggering can lead to a significant reduction in metabolic energy expenditure. Nevertheless, the table indicates that our best optimization result still reaches only 83% of the ultimate bound for energy saving with an extension spring, obtained by assuming perfect storage/release of all available/required mechanical energy in the plot of Figure 5(a). Additional improvement might be possible if one relaxes the periodicity constraint (7) on the release time t_4, which is required for returning the spring's length to its initial value. This relaxation might be possible if the device can be returned to its original state during an "unused" phase. Since this consideration relies on specific details of mechanical implementation of the clutches mechanism, it lies beyond the scope of this work.

Table 5. Summary of optimization stages and energy performance

stage	energy at knee joint [J]	total energy at all joints [J]	% saving knee joint	% saving of total
no spring	343.8	879.7		
spring without clutch timing	330.9	866.8	3.75%	1.47%
naive timing	297.4	833.3	13.5%	5.3%
optimal spring + timing	196.6	732.5	42.8%	16.7%
optimal geometry + spring + timing	181.4	717.3	47.2%	18.5%
ultimate saving (extension spring)	148.7	684.6	56.7%	22.2%

A rather hypothetical way for improving energy performance of the device, which is based on the energy-distance graphs in Figure 5, is to use an arrangement of two devices in parallel, one with a spring in extension and one with a spring in compression. This will enable storing energy at both time intervals $\mathcal{I}_2, \mathcal{I}_3$ and releasing them at $\mathcal{I}_4, \mathcal{I}_1$ respectively, leading (theoretically) to doubled energy saving, whose practical realization might be questionable. Finally, another idea is designing or choosing a *nonlinear spring* with a pre-specified energy profile. Using the gait characteristics in Figure 5, one can construct curves of the potential energy function $U_k(l)$ of a nonlinear spring that will achieve best fit with the desired energy profiles. Note that the potential for mechanical realization of a spring with desired nonlinear behavior must be given careful practical consideration. Thus, this extension also remains as an open challenge for future work.

5. Conclusion

We have theoretically investigated the use of a spring-clutches mechanism with timed triggering for reducing the metabolic energy cost during human walking. We introduced a simple five-link planar model and used kinematic data from motion measurements [39] combined with dynamic equations of motion, in order to obtain the mechanical and metabolic power expenditure at the joints. We introduced a novel concept of a two-clutches mechanism and a linear spring, which enables free motion while the spring is locked with stored elastic energy that can be released at desired stages of the motion. We have presented a series of stages for planning and optimizing the spring properties, clutch timing, and device geometry. The results show a significant reduction in metabolic energy expenditure. This proves that the proposed concept of optimizing a clutch-spring wearable device is theoretically feasible and has a promising potential.

We now briefly discuss some limitations of our theoretical analysis and suggest possible directions for future extensions of the research. First, our five-link planar

model with point feet is obviously an overly simplistic description of human motion. Future generalizations must also account for the foot contact transitions, as well as 3D lateral motions. An immediate extension to a seven-link model that includes ankle joint and a rigid foot based on Winter's classical model [44] is currently under our investigation. This model will enable analysis and performance optimization of a device mounted around the ankle joint as in [22], which cannot be studied using our current point-foot model. Second, our model considers a known fixed kinematic trajectory and a massless device, and does not account for situations where the device's inertia and caused discomfort lead to changes in the gait. Third, our analysis uses the simplistic formula of Margaria [40, 41] for metabolic energy, and future extensions should include more detailed models of muscle activation dynamics and energetics (cf. [45, 46]).

While our analysis studies the spring-clutches mechanism only theoretically, its mechanical design and realization of the triggering mechanism actuation are of fundamental importance and have significant influence on the practical value of this proposed concept. The performance of such a device must be assessed by conducting walking experiments with measurement of metabolic energy expenditure on human subjects under various loading conditions. Finally, a long-term vision of this project is designing of a system for automated optimal tuning of the device based on personalized motion measurements of the walking gait.

Acknowledgments

References

[1] Weiguang Huo, Samer Mohammed, Juan C Moreno, and Yacine Amirat. Lower limb wearable robots for assistance and rehabilitation: A state of the art. *IEEE systems Journal*, 10(3):1068–1081, 2016.

[2] Aaron J Young and Daniel P Ferris. State of the art and future directions for lower limb robotic exoskeletons. *IEEE Transactions on Neural Systems and Rehabilitation Engineering*, 25(2):171–182, 2017.

[3] Larry E Miller, Angela K Zimmermann, and William G Herbert. Clinical effectiveness and safety of powered exoskeleton-assisted walking in patients with spinal cord injury: systematic review with meta-analysis. *Medical devices (Auckland, NZ)*, 9:455, 2016.

[4] David T Bundy, Lauren Souders, Kelly Baranyai, Laura Leonard, Gerwin Schalk, Robert Coker, Daniel W Moran, Thy Huskey, and Eric C Leuthardt. Contralesional brain–computer interface control of a powered exoskeleton for motor recovery in chronic stroke survivors. *Stroke*, 48:116, 2017.

[5] Dennis R Louie and Janice J Eng. Powered robotic exoskeletons in post-stroke rehabilitation of gait: a scoping review. *Journal of neuroengineering and rehabilitation*, 13(1):53, 2016.

[6] HSF White, S Hayes, and M White. The effect of using a powered exoskeleton training programme on joint range of motion on spinal injured individuals: A pilot study. *Int J Phys Ther Rehab*, 1(102):2, 2015.

[7] Katharina Raab, Karsten Krakow, Florian Tripp, and Michael Jung. Effects of training with the ReWalk exoskeleton on quality of life in incomplete spinal cord injury: a single case study. *Spinal cord series and cases*, 2:15025, 2016.

[8] Wayne Yi-Wei Tung, Michael McKinley, Minerva V Pillai, Jason Reid, and Homayoon Kazerooni. Design of a minimally actuated medical exoskeleton with mechanical swing-phase gait generation and sit-stand assistance. In *ASME 2013 Dynamic Systems and Control Conference*, pages V002T28A004–V002T28A004. American Society of Mechanical Engineers, 2013.

[9] Yoshihiro Kusuda. In quest of mobility–honda to develop walking assist devices. *Industrial Robot: An International Journal*, 36(6):537–539, 2009.

[10] Yasushi Ikeuchi, Jun Ashihara, Yutaka Hiki, Hiroshi Kudoh, and Tatsuya Noda. Walking assist device with bodyweight support system. In *Intelligent Robots and Systems, 2009. IROS 2009. IEEE/RSJ International Conference on*, pages 4073–4079. IEEE, 2009.

[11] P Karthikeyan, M Ajin, et al. Geriatric walk assist robot-design, analysis and implementation of a modular lower limb exoskeleton robot. *Applied Mechanics & Materials*, 852, 2016.

[12] Carlo Kopp. Exoskeletons for warriors of the future. *Defence Today*, 9(2):38–40, 2011.

[13] S Jacobsen. On the development of XOS, a powerful exoskeletal robot. In *2007 IEEE/RSJ International Conference on Intelligent Robots and Systems, Plenary Talk*, 2007.

[14] H Kazerooni. Human augmentation and exoskeleton systems in berkeley. *International Journal of Humanoid Robotics*, 4(03):575–605, 2007.

[15] Marco Fontana, Rocco Vertechy, Simone Marcheschi, Fabio Salsedo, and Massimo Bergamasco. The body extender: A full-body exoskeleton for the transport and handling of heavy loads. *IEEE Robotics & Automation Magazine*, 21(4):34–44, 2014.

[16] Robert Bogue. Robotic exoskeletons: a review of recent progress. *Industrial Robot: An International Journal*, 42(1):5–10, 2015.

[17] Warren Cornwall. In pursuit of the perfect power suit. *Science*, 350(6258):270–273, 2015.

[18] Philippe Malcolm, Samuel Galle, and Dirk De Clercq. Fast exoskeleton optimization. *Science*, 356(6344):1230–1231, 2017.

[19] Fausto A Panizzolo, Ignacio Galiana, Alan T Asbeck, Christopher Siviy, Kai Schmidt, Kenneth G Holt, and Conor J Walsh. A biologically-inspired multi-joint soft exosuit that can reduce the energy cost of loaded walking. *Journal of neuroengineering and rehabilitation*, 13(1):43, 2016.

[20] Kamran Shamaei, Massimo Cenciarini, Albert A Adams, Karen N Gregorczyk, Jeffrey M Schiffman, and Aaron M Dollar. Design and evaluation of a quasi-passive knee exoskeleton for investigation of motor adaptation in lower extremity joints. *IEEE Transactions on Biomedical Engineering*, 61(6):1809–1821, 2014.

[21] R.M.N. Alexander. *Elastic Mechanisms in Animal Movement*. Cambridge University Press, 1988.

[22] Steven H Collins, M Bruce Wiggin, and Gregory S Sawicki. Reducing the energy cost of human walking using an unpowered exoskeleton. *Nature*, 522(7555):212–215, 2015.

[23] J Hoover and SA Meguid. Performance assessment of the suspended-load backpack. *International Journal of Mechanics and Materials in Design*, 7(2):111–121, 2011.

[24] Jeffrey Ackerman, Kevin Kelley, and Justin Seipel. Dynamics of carrying a load with a handle suspension. *Journal of biomechanics*, 48(6):1084–1091, 2015.

[25] Jeffrey Ackerman and Justin Seipel. Design of stabilizing arm mechanisms for carrying and positioning loads. *Journal of Mechanical Design*, 137(10):104501, 2015.

[26] Jeffrey Ackerman and Justin Seipel. Energy efficiency of legged robot locomotion with elastically suspended loads. *IEEE Transactions on Robotics*, 29(2):321–330, 2013.

[27] Lawrence C Rome, Louis Flynn, and Taeseung D Yoo. Biomechanics: Rubber bands reduce the cost of carrying loads. *Nature*, 444(7122):1023–1024, 2006.

[28] Matthieu Foissac, Guillaume Y Millet, André Geyssant, Philippe Freychat, and Alain Belli.

Characterization of the mechanical properties of backpacks and their influence on the energetics of walking. *Journal of biomechanics*, 42(2):125–130, 2009.

[29] Jeffrey Ackerman and Justin Seipel. A model of human walking energetics with an elastically-suspended load. *Journal of biomechanics*, 47(8):1922–1927, 2014.

[30] Dejun Li, Tong Li, Qingguo Li, Tao Liu, and Jingang Yi. A simple model for predicting walking energetics with elastically-suspended backpack. *Journal of biomechanics*, 49(16):4150–4153, 2016.

[31] Elliott J Rouse, Luke M Mooney, Ernesto C Martinez-Villalpando, and Hugh M Herr. Clutchable series-elastic actuator: Design of a robotic knee prosthesis for minimum energy consumption. In *Rehabilitation Robotics (ICORR), 2013 IEEE International Conference on*, pages 1–6. IEEE, 2013.

[32] Conor James Walsh, Ken Endo, and Hugh Herr. A quasi-passive leg exoskeleton for load-carrying augmentation. *International Journal of Humanoid Robotics*, 4(03):487–506, 2007.

[33] M Bruce Wiggin, Gregory S Sawicki, and Steven H Collins. An exoskeleton using controlled energy storage and release to aid ankle propulsion. In *Rehabilitation Robotics (ICORR), 2011 IEEE International Conference on*, pages 1–5. IEEE, 2011.

[34] Ken Endo, Daniel Paluska, and Hugh Herr. A quasi-passive model of human leg function in level-ground walking. In *Intelligent Robots and Systems, 2006 IEEE/RSJ International Conference on*, pages 4935–4939. IEEE, 2006.

[35] Rafael R Torrealba, Samuel B Udelman, and Edgar D Fonseca-Rojas. Design of variable impedance actuator for knee joint of a portable human gait rehabilitation exoskeleton. *Mechanism and Machine Theory*, 116:248–261, 2017.

[36] Daniel FB Häufle, MD Taylor, S Schmitt, and H Geyer. A clutched parallel elastic actuator concept: Towards energy efficient powered legs in prosthetics and robotics. In *Biomedical Robotics and Biomechatronics (BioRob), 2012 4th IEEE RAS & EMBS International Conference on*, pages 1614–1619. IEEE, 2012.

[37] Ryan J Williams, Andrew H Hansen, and Steven A Gard. Prosthetic ankle-foot mechanism capable of automatic adaptation to the walking surface. *Journal of biomechanical engineering*, 131(3):035002, 2009.

[38] Yannick Aoustin and AM Formalskii. Strategy to lock the knee of exoskeleton stance leg: Study in the framework of ballistic walking model. In *New Trends in Medical and Service Robots*, pages 179–195. Springer, 2016.

[39] Shu Jiang, Shawanee Partrick, Huihua Zhao, and Aaron D Ames. Outputs of human walking for bipedal robotic controller design. In *American Control Conference (ACC), 2012*, pages 4843–4848. IEEE, 2012.

[40] Rodolfo Margaria. Positive and negative work performances and their efficiencies in human locomotion. *European journal of applied physiology and occupational physiology*, 25(4):339–351, 1968.

[41] Rodolfo Margaria. *Biomechanics and energetics of muscular exercise*. Oxford University Press, USA, 1976.

[42] Roee Keren and Yizhar Or. Energy performance analysis of a backpack suspension system with a timed clutch for human load carriage. submitted 2017. Preprint available HERE.

[43] Richard M Murray, Zexiang Li, S Shankar Sastry, and S Shankara Sastry. *A mathematical introduction to robotic manipulation*. CRC press, 1994.

[44] David A Winter. *Biomechanics and motor control of human movement*. John Wiley & Sons, 2009.

[45] Jack M Winters. Hill-based muscle models: a systems engineering perspective. In *Multiple muscle systems*, pages 69–93. Springer, 1990.

[46] Jing Z Liu, Robert W Brown, and Guang H Yue. A dynamical model of muscle activation, fatigue, and recovery. *Biophysical journal*, 82(5):2344–2359, 2002.